








# Leaf water $\delta^{18}\text{O}$ , $\delta^2\text{H}$ and $d$ -excess isoscapes for Australia using region-specific plant parameters and non-equilibrium vapour

Francesca A. McInerney<sup>1,2,3</sup>  | Christoph Gerber<sup>4</sup>  | Emma Dangerfield<sup>2</sup> |  
 Lucas A. Cernusak<sup>5</sup>  | Athina Puccini<sup>3</sup>  | Steve Szarvas<sup>3</sup>  | Tanoj Singh<sup>6</sup>  |  
 Nina Welti<sup>3</sup> 

<sup>1</sup>School of Earth and Environmental Sciences, University of Queensland, St. Lucia, Queensland, Australia

<sup>2</sup>Department of Earth Sciences, University of Adelaide, Adelaide, South Australia, Australia

<sup>3</sup>Agriculture and Food, Commonwealth Scientific and Industrial Research Organisation, Adelaide, South Australia, Australia

<sup>4</sup>Land and Water, Commonwealth Scientific and Industrial Research Organisation, Adelaide, South Australia, Australia

<sup>5</sup>College of Science and Engineering, James Cook University, Cairns, Queensland, Australia

<sup>6</sup>Agriculture and Food, Commonwealth Scientific and Industrial Research Organisation, Werribee, Victoria, Australia

## Correspondence

Francesca A. McInerney, School of Earth and Environmental Sciences, University of Queensland, St. Lucia, QLD 4072, Australia.  
 Email: [cesca.mcinerney@uq.edu.au](mailto:cesca.mcinerney@uq.edu.au)

Christoph Gerber, Land and Water, Commonwealth Scientific and Industrial Research Organisation, Locked Bag 2, Glen Osmond, 5064, Adelaide, South Australia, Australia.  
 Email: [christoph.gerber@csiro.au](mailto:christoph.gerber@csiro.au)

## Funding information

Science and Industry Endowment Fund

## Abstract

Oxygen ( $\delta^{18}\text{O}$ ) and hydrogen ( $\delta^2\text{H}$ ) isotope ratios, and their relationship to one another ( $d$ -excess) are altered as water travels from the atmosphere to the land surface, into soils and plants and back to the atmosphere. Plants return water to the atmosphere through transpiration (evaporation through the stomata), which causes isotopic fractionation concentrating the heavier isotopes ( $^{18}\text{O}$  and  $^2\text{H}$ ) in the water that remains behind in the leaves. The degree of isotopic fractionation during transpiration is controlled largely by climate, and as a result can be predicted using process-based models and climate data. The modelled transpirational isotopic fractionation can be applied to plant source water isotopic values to predict leaf water isotope ratios and generate maps of isotopic composition, or isoscapes. This approach of mechanistic modelling has been well demonstrated in the first generation of global leaf water isoscapes (*PLoS One*, 3(6), e2447, 2008). However, use of leaf water isoscapes in fields such as hydrology, ecology, and forensics requires a new generation of updated region-specific isoscapes. Here, we generate leaf water isoscapes of  $\delta^{18}\text{O}$ ,  $\delta^2\text{H}$  and  $d$ -excess for Australia, the driest vegetated continent on Earth, where leaf water represents a critical water resource for ecosystems. These isoscapes represent an improvement over previous global isoscapes due to their higher resolution, region-specific, empirically derived plant parameters, and non-equilibrium corrections for water vapour isotopic composition. The new isoscapes for leaf water are evaluated

Francesca A. McInerney and Christoph Gerber should be considered as joint first author.

This is an open access article under the terms of the [Creative Commons Attribution-NonCommercial](https://creativecommons.org/licenses/by-nc/4.0/) License, which permits use, distribution and reproduction in any medium, provided the original work is properly cited and is not used for commercial purposes.

© 2023 The Authors. *Hydrological Processes* published by John Wiley & Sons Ltd.

relative to observed isotope ratios of leaf cellulose and cherry juice. The model predictions for annual average leaf water isotope ratios showed strong correlations with these plant tissues that integrate over time. Moreover, inclusion of region-specific leaf temperature estimates and non-equilibrium vapour corrections improved prediction accuracy. Regionally based isoscapes provide improved characterisations of average leaf water isotope ratios needed to support research in hydrology, plant ecophysiology, atmospheric science, ecology, and geographic provenancing of biological materials.

#### KEYWORDS

Australia, deuterium, isoscapes, leaf water, oxygen

## 1 | INTRODUCTION

Freshwater derives from precipitation over land that can be partitioned into “blue water” and “green water” flows (Rockström & Falkenmark, 2000). Blue water refers to the portion that flows via runoff and rivers into groundwater and the ocean; green water refers to the portion of precipitation that is captured by soils and plants and is returned to the atmosphere as vapour via evaporation and transpiration (evaporation from leaves through stomata) (Rockström & Falkenmark, 2000). Of the precipitation that falls on land, roughly 60% joins the green water path and 40% joins the blue water path globally (Oki & Kanae, 2006). However, because of its much shorter residence time, green water storage as soil moisture and biological water in living organisms makes up only 0.08% of global freshwater storage (Oki & Kanae, 2006). Remarkably, although only a minute fraction of global freshwater storage, green water enables life on land by supporting photosynthesis, ecosystem functioning and rainfed agriculture.

The dependance of life on green water is especially evident in drylands where blue water is limited. Drylands are defined as regions with permanent or seasonal water deficiency and account for 45% of terrestrial landmasses (Průhová, 2016). Drylands support 44% of cultivated systems and 50% of the world's livestock (Davies et al., 2012; UN, 2011). Australia is the most arid continent on earth, with 90% characterized as drylands (Průhová, 2016), and supports globally unique ecosystems with high degrees of endemism (Crisp et al., 2001). Plants in drylands are more sensitive to rainfall pulses than those in mesic environments, exhibiting more frequent and sustained plant carbon and water uptake responses (Feldman et al., 2021). The water taken up by plants from soils in drylands is used not only for plant growth, but also as a source of liquid water for consumers of those plants (Ehleringer et al., 1999). By drawing the water out of the soil and into leaves, plants make a formerly inaccessible water pool available. Many arid adapted herbivores such as Kangaroos and gazelles rely heavily on leaf water as a source of liquid water (Ayliffe & Chivas, 1990; Daniel Bryant & Froelich, 1995; Kohn et al., 1996; Murphy & Bowman, 2007). Thus, leaf water in drylands

represents an important water resource for supporting ecosystem productivity and biodiversity.

Characterizing stable isotopic ratios of leaf water in drylands is essential for being able to trace this important green water pool into ecosystems and agriculture. The environmental parameters that control leaf water isotope ratios are well established and well tested (see Cernusak et al., 2016 for review). During transpiration, leaf water becomes enriched in the heavy isotopes of oxygen ( $^{18}\text{O}$ ) and hydrogen ( $^2\text{H}$ ) relative to the source water taken up by the leaf. The degree of isotopic enrichment relative to source water is influenced most significantly by the relative humidity of the surrounding atmosphere, with a minor effect of temperature (see Figure 1 for schematic of leaf water modelling and methods for detailed description). Comparison of the oxygen and hydrogen isotope ratios of water can be used to determine Deuterium excess (*d*-excess), a measure of the difference in intercept from the global meteoric water line (GMWL) (Dansgaard, 1964). The *d*-excess of leaf water reflects climatic conditions surrounding the leaf and has been shown to influence the *d*-excess values of atmospheric moisture (Zongxing et al., 2016; Simonin et al., 2014; Zhao et al., 2014).

Spatial variations in the isotopic signatures of leaf water can be modelled and mapped as isoscapes. These predictive isoscapes enable examination of isotopic patterns without requiring large reference collections from remote regions, which can be difficult and expensive to generate. Global isoscapes of leaf water have demonstrated the potential of mechanistic models for predicting variations in leaf water oxygen and hydrogen isotope ratios at large spatial scales (West et al., 2008; Woo et al., 2021), but required simplifications that can introduce uncertainties at finer geographic scales. To apply isotope tracers to ecohydrological and forensic questions at more local scales requires high-resolution, regionally calibrated isoscapes. Regional specificity can be achieved by using empirical calibrations for the plant-based parameters of leaf temperature and kinetic fractionation during diffusion through the stomata and the leaf boundary layer ( $\epsilon_k$ ) (Figure 1). Moreover, recent advances in quantifying the non-equilibrium nature of atmospheric water vapour (Fiorella et al., 2019) and its influence on leaf water isotope ratios (Cernusak et al., 2022)

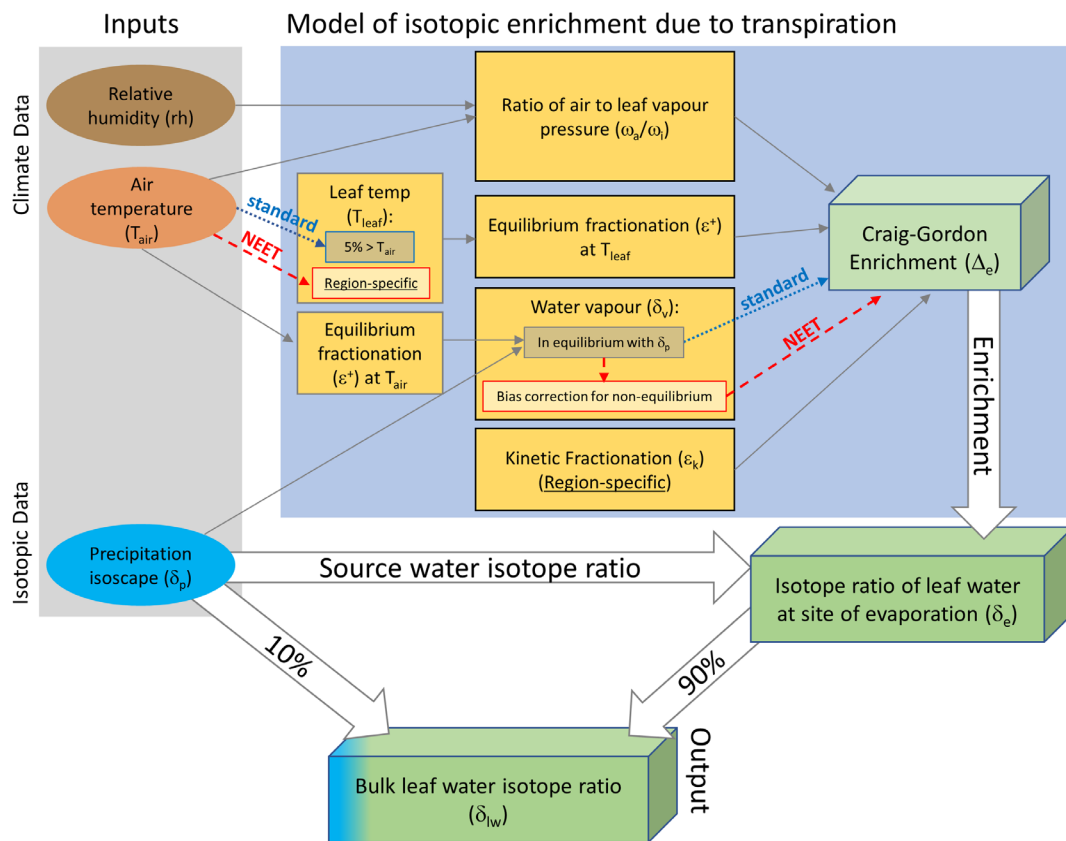


**FIGURE 1** Schematic illustrating the leaf water model inputs, parameters and outputs used to develop bulk leaf water isoscapes. Two model options are illustrated: ‘standard’ and ‘non-equilibrium, empirical temperature’ (NEET), with the differences between them indicated. Region-specific empirical estimates of plant parameters (leaf–air temperature relationship and kinetic fractionation) are indicated with underlining.

present the opportunity to correct for non-equilibrium vapour to improve leaf water modelling (Figure 1).

Here we develop leaf water isoscapes for Australia that employ regionally modelled precipitation isotope inputs, regionally calibrated plant parameters, relevant climate data, and non-equilibrium atmospheric vapour isotope ratios. The leaf water model used here (Figure 1) uses precipitation isoscapes from Hollins et al. (2018) that are based on more than twice as many Australian sampling locations (15 stations) as previously available in the global models (7 Australian stations; Bowen, 2010a, 2010b; Bowen & Revenaugh, 2003) with greater sampling of inland Australia. The plant parameters of kinetic fractionation and leaf temperature are empirically estimated from measurements from across Australia (Cernusak et al., 2016, 2022; Munksgaard et al., 2017). Relative humidity inputs are limited to day-time values to best represent periods of transpiration; rather than 24 h values as were previously used for relative humidity (West et al., 2008). Water vapour has frequently been assumed to be in isotopic equilibrium with precipitation (Gat, 2000; West et al., 2008). While equilibrium can occur during sufficiently long rainfall events, atmospheric vapour is not generally in equilibrium with local annual precipitation on longer timescales (Fiorella et al., 2019; Welp et al., 2008). Recent estimates of the degree of disequilibrium around the globe (Fiorella et al., 2019) enable correction for the disequilibrium of water vapour. Water vapour isotopic composition has a large effect on the hydrogen isotope ratio

and *d*-excess of leaf water (Cernusak et al., 2022), making proper estimation critical to accurate development of leaf water isoscapes.

The isoscapes developed here, like the global leaf water isoscapes (West et al., 2008), use process-based models to predict isotope ratios. This is in contrast to geostatistical approaches to predict values and/or interpolate between observations (Bowen, 2010a, 2010b; Woo et al., 2021). This mechanistic approach is critical for leaf water prediction because leaf water isotope ratios are highly variable spatially and temporally. Short-term fluctuations in source water, climate and transpiration rate lead to fluctuations in leaf water isotope ratios within a day, within an individual plant and within a leaf (Cernusak et al., 2016). As a result, geostatistical models applied to relatively small datasets of instantaneous leaf water observations will not generate reliable isoscapes of average bulk leaf water. Yet, time-integrated average bulk leaf water is the relevant measure when examining plant and animal materials that develop over time. By employing process based models (Figure 1) that reliably predict short-term observations (Cernusak et al., 2016) with long-term average climatic and isotopic inputs, we can develop average leaf water isoscapes that are relevant for ecohydrology, atmospheric science, agriculture and forensics.

The aims of this study are to

1. develop leaf water isoscapes for Australia that draw on region-specific information and account for vapour disequilibrium;

2. quantify differences between the new Australian leaf water isoscapes and for hydrogen (Horita & Wesolowski, 1994) as

$$\alpha^+ = \text{EXP} \left[ \frac{\left( 1158.8 \cdot \left( \frac{(T+273.15)^3}{10^9} \right) - 1620.1 \cdot \left( \frac{(T+273.15)^2}{10^6} \right) + 794.84 \cdot \left( \frac{T+273.15}{10^3} \right) - 161.04 + 2.9992 \cdot \left( \frac{10^9}{(T+273.15)^3} \right) \right)}{1000} \right]. \quad (4)$$

scapes and the previous global isoscapes, and attribute these differences to specific model parameters;

3. evaluate whether regional inputs improve the accuracy of these new isoscapes for predicting isotope ratios of plant materials, namely fruit juice and leaf cellulose.

## 2 | DATA AND METHODS

### 2.1 | Leaf water modelling

The oxygen and hydrogen isotope enrichment caused by transpiration can be estimated using a modified Craig-Gordon model with two-pool mixing to determine steady-state bulk leaf water isotope ratios as illustrated in Figure 1 (Cernusak et al., 2016).

The modified Craig-Gordon model estimates the isotopic enrichment of leaf water above source water at the site of evaporation ( $\Delta_e$ ) (Cernusak et al., 2016; Craig & Gordon, 1965) and is expressed in per mil (‰) as:

$$\Delta_e = \left[ \left( 1 + \frac{\epsilon^+}{1000} \right) \cdot \left( \left( 1 + \frac{\epsilon_k}{1000} \right) \cdot \left( 1 - \frac{\omega_a}{\omega_i} \right) + \frac{\omega_a}{\omega_i} \cdot \left( 1 + \frac{\Delta_v}{1000} \right) \right) - 1 \right] \cdot 1000 \quad (1)$$

where  $\epsilon^+$  is the equilibrium fractionation between liquid water and vapour,  $\epsilon_k$  is the kinetic fractionation for combined diffusion through the stomata and the boundary layer,  $\omega_a/\omega_i$  is the ratio of the water vapour mole fraction in the air relative to that in the intercellular air spaces (with  $\omega_i$  assumed to be at saturation), and  $\Delta_v$  is the isotopic enrichment of atmospheric vapour compared to source water.

The equilibrium fractionation ( $\epsilon^+$ ) in per mil (‰) is related to the equilibrium fractionation factor ( $\alpha^+$ ) as

$$\epsilon^+ = (\alpha^+ - 1) \cdot 1000. \quad (2)$$

The equilibrium fractionation factor ( $\alpha^+$ ) depends on temperature ( $T$ ) and is calculated for the temperature at the leaf surface ( $T_{\text{leaf}}$ ) in degrees Celsius for oxygen (Horita & Wesolowski, 1994) as

$$\alpha^+ = \text{EXP} \left[ \frac{-7.685 + 6.7123 \cdot \left( \frac{10^3}{T+273.15} \right) - 1.6664 \cdot \left( \frac{10^6}{(T+273.15)^2} \right) + 0.35041 \cdot \left( \frac{10^9}{(T+273.15)^3} \right)}{1000} \right], \quad (3)$$

The isotopic enrichment of water vapour relative to source water ( $\Delta_v$ ) is calculated as

$$\Delta_v = \frac{\delta_v - \delta_p}{1 + \frac{\delta_p}{1000}} \quad (5)$$

where  $\delta_v$  is the isotopic composition of atmospheric water vapour and  $\delta_p$  is the isotopic composition of precipitation in per mil (‰).

The modified Craig-Gordon equation ( $\Delta_e$ ) (Equation 1) simulates the isotopic enrichment relative to source water values. Using precipitation isotope ratios ( $\delta_p$ ) for source water isotope ratios, the isotopic composition of leaf water at the site of evaporation ( $\delta_e$ ) can be estimated as

$$\delta_e = \left( \Delta_e \cdot \left( 1 + \frac{\delta_p}{1000} \right) + \delta_p \right). \quad (6)$$

Bulk leaf water isotopic values are generally lower than the Craig-Gordon approximation due to the Peclet effect and mixing of unenriched source water with enriched water from the site of evaporation (see Cernusak et al., 2016 for review). To adjust for these effects, bulk leaf water can be estimated using two-pool mixing between water from the site of evaporation and source water (Barbour et al., 2021; Cernusak et al., 2016; Leaney et al., 1985; West et al., 2008). Bulk leaf water is estimated here using a mixing ratio of 90% enriched leaf water and 10% source water, which best matches empirical observations (Cernusak et al., 2016; Song et al., 2015).

$$\delta_{\text{lw}} = 0.1 \cdot \delta_p + 0.9 \cdot \delta_e \quad (7)$$

From the hydrogen and oxygen isotope ratios of leaf water,  $d$ -excess for leaf water was calculated as follows (Dansgaard, 1964).

$$d\text{-excess} = \delta^2\text{H}_{\text{lw}} - 8 \cdot \delta^{18}\text{O}_{\text{lw}} \quad (8)$$

## 2.2 | Model input parameters

All leaf water model calculations were conducted in R and the code is available in Supporting Information. The input data and parameter estimations are as follows.

### 2.2.1 | Air temperature

Several temperature grids interpolated from measured data from 600 weather stations using the approach described in Jones et al. (2009) were obtained from the Australian Bureau of Meteorology (BoM, 2005): (a) Long term averages for the period from 1976 to 2005 for 9 am and 3 pm at a resolution of 0.05° (~5 km, Figure 2a). A daytime mean temperature was calculated by averaging the 9 am and 3 pm values and used for annual isoscape modelling. This grid was used as the base grid to which all other gridded data was adjusted. (b) Monthly long-term averages for the period 1961 to 1990 of daily mean temperature at a resolution of 0.025° (~2.5 km, BoM, 2005). Daytime mean temperature was estimated by adding an offset of 2.5°C to the daily mean temperature (Lloyd & Farquhar, 1994). Monthly values were used to explore intra-annual variations in predicted leaf water isotope ratios.

### 2.2.2 | Relative humidity

Relative humidity (RH) grids interpolated from measured data from 530 weather stations using the ANU 3-D Spline surface-fitting algorithm were obtained from the Australian Bureau of Meteorology (BoM, 2009). All grids are long-term averages for the period from 1976 to 2005 with a resolution of 0.1° (~10 km) and were disaggregated by a factor of 2 to match the temperature grid. As for temperature, annual 3 pm and 9 am grids, as well as monthly 3 pm and 9 am grids were available. For the annual grids, we calculated daytime averages by converting the 9 am and 3 pm RH to vapour pressure, averaging the vapour pressure grids, and converting back to RH (Figure 2b), but found the difference to simply averaging the two RH grids was generally less than 1 percentage point.

### 2.2.3 | Leaf temperature

Leaf temperature was estimated in two different ways. In the standard model, leaf temperature ( $T_{\text{leaf}}$ ) was calculated as 5% higher than daytime air temperature  $T_{\text{air}}$ , following the classical approach by Lloyd and Farquhar (1994) and as in the previous global modelling (West et al., 2008). However,  $T_{\text{leaf}}$  can be lower than  $T_{\text{air}}$  due to leaf-temperature homeostasis (Dong et al., 2017). Therefore, in a second model, termed 'non-equilibrium, empirical temperature' (NEET), an empirical relationship was used based on Australian published observations of leaf and air temperature (SI Figure S2; 229 data points;

Cernusak et al., 2016, 2022; Munksgaard et al., 2017), with a result similar to Munksgaard et al. (2017):

$$T_{\text{leaf}} = 0.94 + 0.94 \cdot T_{\text{air}} \quad (9)$$

### 2.2.4 | Isotopic composition of atmospheric water vapour

The isotopic composition of atmospheric water vapour ( $\delta_v$ ) was estimated in two different ways in the standard and NEET models. In the standard model, isotopic equilibrium was assumed between precipitation and water vapour and  $\epsilon^+$  and  $\alpha^+$  were calculated using the average daytime air temperature and Equations (2)–(4) (Horita & Wesolowski, 1994). This is the same assumption made in the global isoscapes (West et al., 2008). Vapour isotopic composition in equilibrium with precipitation was calculated as follows.

$$\delta_v = \frac{\delta_p - \epsilon^+}{\alpha^+} \quad (10)$$

However, atmospheric vapour is not generally in isotopic equilibrium with local annual precipitation, and recent modelling has estimated the spatially resolved offset of vapour from equilibrium (Fiorella et al., 2019). Therefore, in the NEET model, the oxygen and hydrogen isotopic ratios of vapour were bias corrected for non-equilibrium based on estimations of Fiorella et al. (2019). Bilinear interpolation was used to convert the original data with a resolution of 2° × 2° (SI Figure S1) to a grid that matches the other grids used here (Figure 2e).

### 2.2.5 | Kinetic fractionation

Kinetic fractionation due to diffusion from the interior of the leaf, through the stomatal pores and then the boundary layer to the atmosphere is described by  $\epsilon_k$ . Because kinetic fractionation through stomata and boundary layer differs, the overall kinetic fractionation depends on the relative contributions of the resistances of the stomata and boundary layer to the overall resistance (Farquhar et al., 1989). Here, we use isotopic fractionation values of 28‰ for oxygen and 25‰ for hydrogen for diffusion through the stomata (Merlivat, 1978), with corresponding values for the leaf boundary layer of 19‰ and 17‰, respectively (Farquhar et al., 1989). Overall values for  $\epsilon_k$  were calculated from measurements of stomatal resistance in the field and estimates of boundary layer resistance from windspeed and leaf size of broad, needle and phyllode leaf-type plants across Australia (Cernusak et al., 2016; Cernusak et al., 2022; Munksgaard et al., 2017). To obtain representative values across diurnal climate fluctuations, values for  $\epsilon_k$  were averaged for each observational day, site and species, yielding 51 separate estimates. For this study, we used the mean of these estimates as a fixed value of  $\epsilon_k$  across all of Australia (26.9 ± 0.5‰ for oxygen and 23.9 ± 0.5‰ for hydrogen).

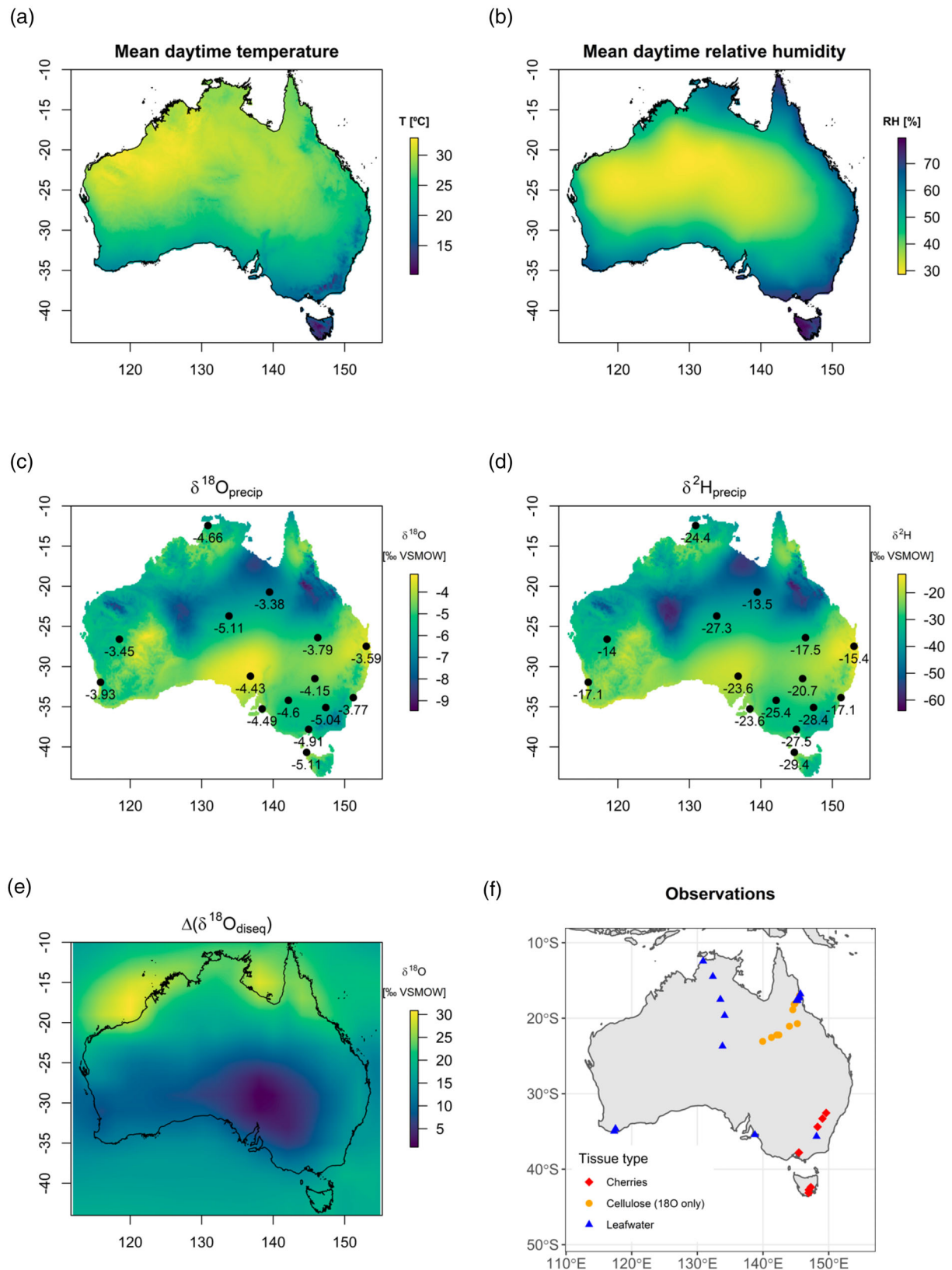


**FIGURE 2** Climate and isotopic data inputs for leaf water model and map of locations for observational data for comparison with models: Climate rasters of 30 year normal for mean daytime air temperature (a) and mean daytime relative humidity (b) from the Bureau of Meteorology; Precipitation isoscapes for oxygen (c) and hydrogen (d) with precipitation sampling locations and average site values indicated, from Hollins et al., 2018; Non-equilibrium correction for atmospheric water vapour for  $\delta^{18}\text{O}$  (e), interpolated from Fiorella et al., 2019 to match the resolution of the climate data (Note: the correction for  $\delta^2\text{H}$  has the same spatial pattern with an eight-fold larger magnitude; see SI Figure S1); Sampling locations for observations of leaf water (blue; from Cernusak et al., 2022; Cernusak et al., 2016; Munksgaard et al., 2017), leaf cellulose (orange; from Cheesman & Cernusak, 2017), cherries (red; from Stockmann et al., 2021) (f).

The previous global model (West et al., 2008) used values for diffusion through stomata of 32‰ for oxygen and 16.4‰ for hydrogen and the associated values for diffusion through the leaf boundary layer of 21‰ and 11‰ for oxygen and hydrogen, respectively (Cappa et al., 2003). We have chosen the Merlivat (1978) values for diffusive fractionation through stomata because these were confirmed to be more appropriate (Luz et al., 2009) after the publication of West et al. (2008). West et al. (2008) used spatially variable conductances for the calculation of  $\epsilon_k$ . Assuming representative values for stomatal and boundary layer conductances for Australia, we estimate that the  $\epsilon_k$  values in the West et al. (2008) analysis for comparison with ours would have been roughly 31.2‰ for oxygen and 16.0‰ for hydrogen.

## 2.2.6 | Oxygen and hydrogen isotope ratios of precipitation

The  $\delta^{18}\text{O}$  and  $\delta^2\text{H}$  values for precipitation for Australia were derived from the annual average isoscapes of Hollins et al. (2018). These isoscapes are based on measured  $\delta^{18}\text{O}$  and  $\delta^2\text{H}$  ratios from 15 sampling locations (Figure 2c,d) and incorporate regional meteorology and geography for interpolation. These isoscapes have a resolution of approximately 10 km. Bilinear interpolation was used to create a grid that is equivalent to the grid of the climate data (5 km resolution).

## 2.3 | Plant isotope ratios for evaluating accuracy of model predictions

### 2.3.1 | Observations of leaf water isotope ratios

Data on oxygen and hydrogen isotope ratios of leaf water and xylem water for plants from 14 sampling sites around Australia (Figure 2f), and associated instantaneous climate measurements were compiled in Cernusak et al. (2016), Cernusak et al. (2022) and Munksgaard et al. (2017). The data was collected during the day, between the hours of 8 am to 5 pm, in the months of March, April, September, November or December, from 2000 to 2010 (For detailed sampling methods, see original publications: Cernusak et al., 2016, 2022; Munksgaard et al., 2017). Values of several hundred observations were averaged for each site, species and day of observation, yielding 51 unique values that were also used for estimates for  $\epsilon_k$  (see Section 2.2.5) and for the leaf-air temperature relationship (Equation (8); SI Figure S2). The original publications (Cernusak et al., 2016; 2022; Munksgaard et al., 2017) demonstrated a good agreement between observations and Craig-Gordon predictions using short-term climate and xylem water isotope ratios. To confirm that the standard and NEET models used here accurately represent the key processes that determine leaf water isotope ratios, predictions were made using short-term climate observations and measured xylem water isotope values as inputs (Cernusak et al., 2016, 2022; Munksgaard et al., 2017) and compared with observations. Observations were also compared with long-term

average predictions of the NEET model based on annual average climate and precipitation isoscapes (Hollins et al., 2018) as inputs.

### 2.3.2 | Measurements of cherry juice isotope ratios

Data on cherry juice isotope ratios were compiled in Stockmann et al., 2021. Cherries were sampled from commercial cherry orchards in the major cherry growing regions of New South Wales, Victoria and Tasmania (Figure 2f). The cherries were of the Lapin variety for all but one site (Mudgee) where the Simone variety was sampled. Samples of ~500–1000 g of bulk cherries were sourced from 33 single trees during the cherry harvest period in December 2018 and January 2019. Fresh cherries were frozen immediately and stored frozen until laboratory analysis.

Frozen cherry samples were thawed slowly at 4°C and wiped to remove any condensed atmospheric moisture. Cherry pits were removed and 200 g of the remaining fruit was turned to a pulp. Fruit pulp was pelletized using a centrifuge and the supernatant was decanted. A subsample of 20 mL was filtered through 0.22  $\mu\text{m}$  filter. To each sample, ethanol (99% AR grade) was added to reach 10% of final solution to prevent fermentation.

A 200 mL aliquot of cherry fruit water was taken and equilibrated for a minimum of 18 h with 10%  $\text{CO}_2$  gas at approximately  $30 \pm 1^\circ\text{C}$ . The  $\delta^{18}\text{O}$  of the equilibrated  $\text{CO}_2$  gas was then analysed with a gas bench coupled to a Delta V mass spectrometer (Thermo Electron Co, Germany).  $\text{CO}_2$  rapidly equilibrates with water and has been shown to reflect accurately the  $\delta^{18}\text{O}$  of water in water/ethanol mixtures (Houderou et al., 1999; Koziat et al., 1995).

### 2.3.3 | Observations of leaf cellulose isotope ratios

Published oxygen isotope ratios of leaf cellulose from *Eucalyptus* trees for 11 sites in Queensland (Figure 2f) were reported in Cheesman and Cernusak (2017) and used here for evaluating the accuracy of the leaf water isoscape predictions.

## 2.4 | Effect of differences in input parameterizations on leaf water isoscapes

The previous global isoscapes (West et al., 2008) and the two models developed here (standard and NEET) vary in numerous ways (Table 1). Extra model runs were done where one or two input parameterizations were replaced with different parameterizations in order to investigate the effect of differences in input parameters by comparing pairs of model runs (Table 2). Difference maps of model pairs were used to explore spatial effects of input parameters and the distribution of differences were used to evaluate the relative contributions of input parameters to the overall difference between different models. Pairwise differences were calculated as Model 1–Model 2 (Table 2).

**TABLE 1** Comparison of leaf water isoscape models investigated here.

Variable/parameter	Global model (West et al., 2008)	Standard model	NEET model
Air temperature	"10' climatology" monthly gridded data from New et al. (2002). Daytime temperature estimated following Hoffmann et al. (2004).	Bureau of Meteorology 9 am and 3 pm air temperature interpolated from 600 weather stations. Daytime temperature as average of 9 am and 3 pm.	Bureau of Meteorology 9 am and 3 pm air temperature interpolated from 600 weather stations. Daytime temperature as average of 9 am and 3 pm.
Relative humidity	Daily (24 h) average relative humidity from New et al. (2002) based on <100 stations.	Bureau of Meteorology 9 am and 3 pm relative humidity interpolated from >500 weather stations.	Bureau of Meteorology 9 am and 3 pm relative humidity interpolated from >500 weather stations.
Precipitation isoscape	Bowen and Revenaugh (2003) based on 7 Australian sampling locations	Hollins et al. (2018) based on 15 Australian sampling locations	Hollins et al. (2018) based on 15 Australian sampling locations
Leaf temperature	5% higher than air temperature	5% higher than air temperature	Mostly cooler than air temperature based on empirical calibration for Australia
Water vapour isotopic composition	Assumes equilibrium with precipitation isotope ratios at daytime air temperature.	Assumes equilibrium with precipitation isotope ratios at daytime air temperature.	Corrected for non-equilibrium effects from Fiorella et al. (2019).
Kinetic fractionation ( $\epsilon_k$ )	Spatially variable, with representative values for Australia of 31.2‰ and 16.0‰ for $\delta^{18}\text{O}$ and $\delta^2\text{H}$ , respectively	Fixed: 26.9‰ and 23.9‰ for $\delta^{18}\text{O}$ and $\delta^2\text{H}$ , respectively	Fixed: 26.9‰ and 23.9‰ for $\delta^{18}\text{O}$ and $\delta^2\text{H}$ , respectively
Grid cell size	0.167° (~17 km)	0.05° (~5 km)	0.05° (~5 km)

**TABLE 2** Model pairs compared to investigate the effect of differences in individual input parameterizations.

Parameter effect	Model 1	Model 2
$\epsilon_k$	Standard	Standard, but using best estimate of $\epsilon_k$ used by West et al. (2008)
Precipitation isoscapes	Standard	Standard, but using precipitation isoscapes from West et al. (2008)
Climate (T & RH)	Standard, but with $\epsilon_k$ & precipitation isoscapes from West	West et al. (2008)
Empirical leaf temperature and atmospheric vapour isotopic composition	NEET	Standard

Note: "West" refers to the global isoscapes published in West et al. (2008) and input parameters used therein. Standard and NEET refer to the models calculated in this publication (see Table 1 for detailed descriptions of differences). The comparisons have been calculated for the Craig-Gordon 2-pool models, that is,  $\delta_{\text{lw}}$ .

To explore the effect of using long-term average climate and source water inputs rather than measured values on the accuracy of leaf water predictions as compared to leaf water observations, the NEET model was run using actual and gridded source water and climate inputs, and all possible combinations of source water and climate inputs. Both annual and monthly average gridded climate data

were included to examine if using long-term average climate data for the month of collection improved predictions. Each set of predictions was compared with observations and the model performance was evaluated in terms of RMSE,  $r^2$ , bias, and slope.

### 3 | RESULTS

#### 3.1 | Australian-specific leaf water isoscapes

Modelled leaf water isotopic enrichments at the site of evaporation ( $\Delta_e$ ) for oxygen were smaller for the NEET model, ranging from 9.9‰ to 26.0‰ (median = 21.0‰), than the standard model that ranged from 8.8‰ to 26.5‰ (median 21.9‰; Figure S3). For hydrogen,  $\Delta_e$  was larger for the NEET model, ranging from 39‰ to 76‰ (median = 64‰) than the standard model that ranged from 28‰ to 72‰ (median = 60‰) (Figure S3). For both models, the smallest enrichments were in western Tasmania where relative humidity is the highest and the largest were in the interior of the continent where relative humidity is the lowest.

Isotopic composition of bulk leaf water ( $\delta_{\text{lw}}$ ) in the NEET model ranged from 2.5‰ to 19.0‰ for oxygen and -18‰ to 45‰ for hydrogen (Figure 3a,b). While the general pattern was of increasing values inland relative to the coasts, greater spatial heterogeneity was evident in  $\delta_{\text{lw}}$  than  $\Delta_e$  because of the heterogeneity in precipitation isotope inputs (Figure 2c,d).

Estimations of  $d$ -excess in the NEET model ranged from -22‰ to -114‰ (Figure 3c) with the least negative values in Tasmania and the most negative values in the interior of the continent, a pattern that closely mimics relative humidity (Figure 2b).



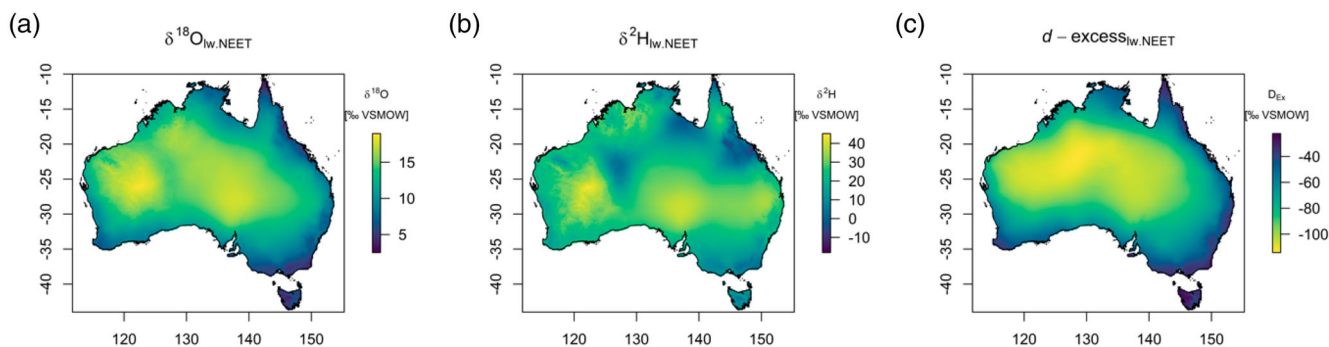


**FIGURE 3** Leaf water isoscapes using the NEET model for (a)  $\delta^{18}\text{O}_{\text{lw}}$ , (b)  $\delta^2\text{H}_{\text{lw}}$ , (c)  $d$ -excess.

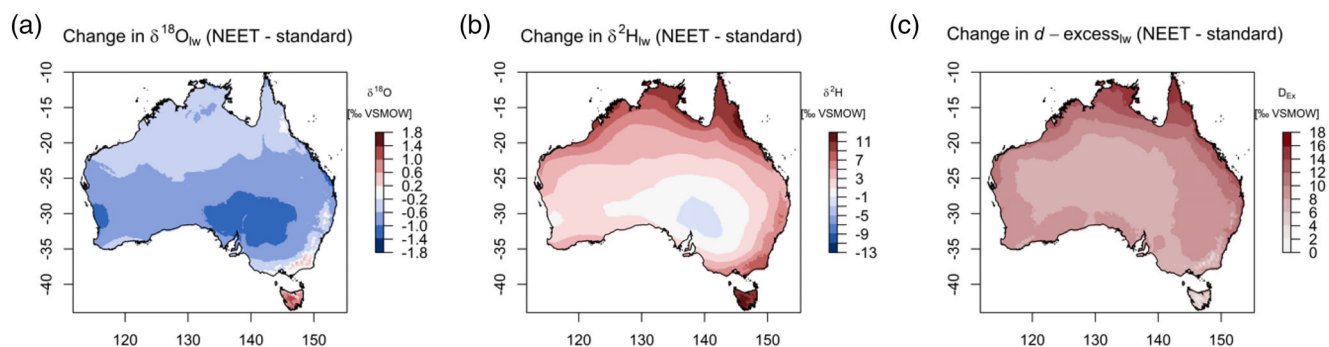


**FIGURE 4** Differences between predicted values from the NEET and standard models for (a)  $\delta^{18}\text{O}_{\text{lw}}$ , (b)  $\delta^2\text{H}_{\text{lw}}$  and (c)  $d$ -excess.

The effects of the differences in assumptions between the NEET and standard models were evaluated by mapping the differences between leaf water isoscapes (Figure 4). The two models showed small differences in oxygen isotope ratios (median difference:  $-0.7\text{‰}$ ; range:  $-1.2\text{‰}$  to  $+1.4\text{‰}$ ; Figure 4a) and larger differences in hydrogen isotope ratios (median difference:  $+2.8\text{‰}$ ; range:  $-1.7\text{‰}$  to  $12.9\text{‰}$ ) and  $d$ -excess (median differences:  $+8.3\text{‰}$ ; range:  $1.5\text{‰}$  to  $16.3\text{‰}$ ) (Figure 4b,c).

The seasonal differences in leaf water isotope ratios for the NEET model were compared through difference maps by subtracting a winter month (July) from a summer month (January) (SI Figure S4). The summer-rainfall dominated north shows negative values and the winter-rainfall dominated south shows positive values. Seasonal differences in  $d$ -excess were inverted relative to  $\delta_{\text{lw}}$ , with the negative differences in the south and positive differences in the north.

The difference between the maximum and minimum monthly values for each grid cell in the NEET model ranged from  $1.7\text{‰}$  to  $11.8\text{‰}$  for oxygen and  $4\text{‰}$  to  $29\text{‰}$  for hydrogen with the highest differences in northern, southwestern and southeastern Australia (SI Figure S5).

While annual and monthly modelling was conducted using the daytime climate (combined 9 am and 3 pm values), we also examined the variability between 9 am or 3 pm NEET model estimates. Table 3 summarizes the spatial and temporal variations in  $\delta_{\text{lw}}$  predicted using the NEET model. Spatial variation is estimated as the width of the

**TABLE 3** Spatial and temporal variations in  $\delta_{\text{lw}}$  using the non-equilibrium, empirical temperature (NEET) model.

	Spatial variation	Seasonal variation	Daily variation
$\delta^{18}\text{O}$	12‰	7‰	5‰
$\delta^2\text{H}$	36‰	17‰	7‰
$d$ -excess	75‰	41‰	32‰

Note: Details of how the values were calculated are provided in the main text.

range encompassing 95% of the grid cell values across all of Australia. For temporal variation (seasonal and daily), the temporal variation was first calculated for each grid cell (i.e., the maximum difference between any 2 months/daytimes for that grid cell). The value reported here is the median of the temporal variation in each grid cell across Australia. Generally, spatial variation across Australia is approximately a factor of two larger than temporal variation between seasons or over a day.

### 3.2 | Comparison of Australian and global leaf water isoscapes

Overall net differences between the standard model and the global isoscapes (West et al., 2008) and the contributions of individual

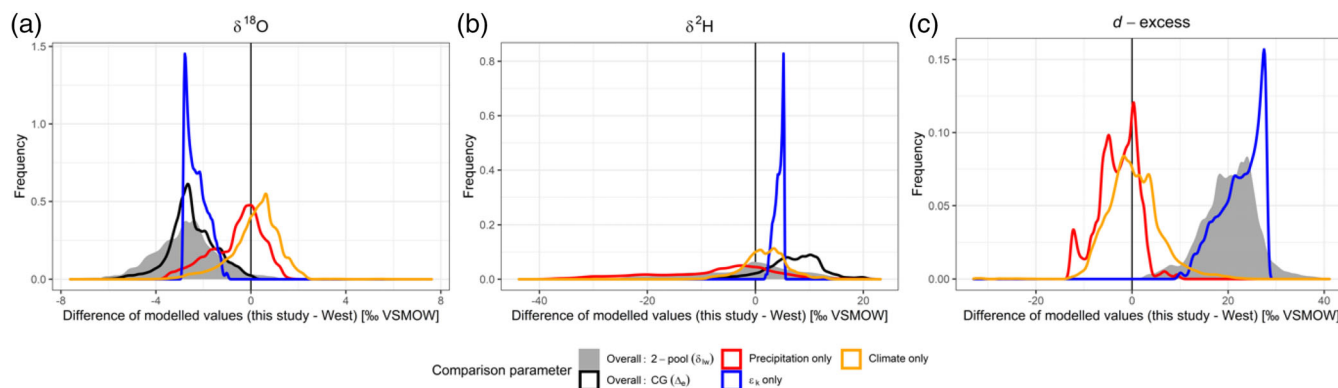


**FIGURE 5** Differences between the standard Australian isoscapes and previous global isoscapes (West et al., 2008) for (a)  $\delta^{18}\text{O}_{\text{lw}}$ , (b)  $\delta^2\text{H}_{\text{lw}}$  and (c)  $d$ -excess. Frequency distributions show the overall differences in 2-pool leafwater isoscapes  $\delta_{\text{lw}}$  (grey) and isotopic enrichment (Craig-Gordon enrichment only)  $\Delta_e$  (black). The contribution of different factors was evaluated by calculating models that differ in the parameterization of input parameters (see Table 2) to isolate the effects of differences in precipitation isotope ratios (red), climate (orange) and kinetic fractionation ( $\epsilon_k$ ) (blue) between West et al. (2008) and this study.

factors to net differences are displayed as frequency distributions (Figure 5), while spatial patterns of net difference and their components are represented by difference maps (Figure S6). The net differences between this study and the global bulk leaf water ( $\delta_{\text{lw}}$ ) isoscapes are shown in shaded grey in Figure 5, with mean ( $\pm$  standard deviation) of  $-2.7 \pm 1.3\text{‰}$  for oxygen,  $0 \pm 9\text{‰}$  for hydrogen and  $21 \pm 6\text{‰}$  for  $d$ -excess.

The spatial variations in the difference between the standard Australian and global isoscapes stems predominantly from differences in the precipitation isotopic inputs. This is evident from the similar spatial patterns in the overall differences (SI Figure S6a–c) and the differences due only to the precipitation isoscapes (SI Figure S6d–f). However, over the entire Australian continent, the use of different precipitation isoscapes only results in minor overall average differences of  $-0.4 \pm 1.0\text{‰}$  for oxygen,  $-5 \pm 11\text{‰}$  for hydrogen, and  $-2.6 \pm 4.1\text{‰}$  for  $d$ -excess (red lines; Figure 5).

The Craig-Gordon enrichment at the site of evaporation ( $\Delta_e$ ) is independent of the isotopic composition of the source water and reflects the combined effects of differences in model structure and differences between the climate and kinetic fractionation inputs, with average differences of  $-2.6 \pm 1.0\text{‰}$  for oxygen and  $+8 \pm 5\text{‰}$  for hydrogen (black lines; Figure 5).

Differences due to climate (different data source with different resolution, but also different ways of calculating effective air and leaf temperatures), showed some spatial coherency among the three isoscapes (SI Figure S6g–i) but contributed only modest differences overall of  $0.3 \pm 1.0\text{‰}$  for oxygen,  $2 \pm 4\text{‰}$  for hydrogen, and  $0 \pm 6\text{‰}$  for the  $d$ -excess (orange lines; Figure 5).

Differences in the values used for kinetic fractionation ( $\epsilon_k$ ), caused differences between the standard and global models of  $-2.4 \pm 0.4\text{‰}$  for oxygen,  $4.5 \pm 0.8\text{‰}$  for hydrogen, and  $23 \pm 4\text{‰}$  for the  $d$ -excess (blue lines; Figure 5). The effects of  $\epsilon_k$  differences were coherent spatially but not constant (SI Figure S6j–l) because of the non-linear nature of Equation (1).

### 3.3 | Model validation

Leaf water isotope predictions from the standard and NEET models using field scale, short-term measured climate data and xylem water isotope ratio inputs (Cernusak et al., 2016, 2022; Munksgaard et al., 2017) are compared to leaf water isotope observations in Figure 6. Predictions using field scale inputs show similar level of accuracy as in the original publications in which individual  $\epsilon_k$  values, rather than average values were used (RMSE of  $<4\text{‰}$  for  $\delta^{18}\text{O}_{\text{lw}}$ ,  $<16\text{‰}$  for  $\delta^2\text{H}_{\text{lw}}$  and  $<26\text{‰}$  for  $d$ -excess). As expected, the instantaneous measurements of leaf water are poorly correlated with long-term average leaf water values modelled using long-term, annual average gridded climate data, producing RMSE values roughly double that of predictions based on field scale inputs (Figure 6).

An assessment of the predictions using the NEET model with different combinations of actual (measured) versus gridded source water and climate inputs is shown in Figure 7. For  $\delta^{18}\text{O}_{\text{lw}}$ , predictions using actual climate data were significantly better than monthly and annual gridded climate data (lower RMSE, higher  $r^2$ ) but there was little effect of using actual rather than annual gridded source water inputs (Figures 6 and 7). In contrast, for  $\delta^2\text{H}_{\text{lw}}$ , performance was vastly improved with the use of measured actual source (xylem) water rather than annual gridded source water inputs (lower RMSE, higher  $r^2$ , lower bias, and slope closer to one) but was only slightly improved with the use of actual rather than gridded climate inputs (Figure 7). For  $d$ -excess, performance with regards to RMSE and  $r^2$  was most improved with the use of actual versus gridded climate but showed little effect of using actual versus gridded source water inputs. However, using actual source water inputs reduced the bias of the  $d$ -excess predictions. Using monthly rather than annual gridded long-term average climate data led to slightly improved model performance for  $\delta^{18}\text{O}_{\text{lw}}$  and  $d$ -excess but had little effect on performance for  $\delta^2\text{H}_{\text{lw}}$ . Overall, predictions of  $\delta^{18}\text{O}_{\text{lw}}$  and  $d$ -excess were most sensitive to climate inputs while predictions of hydrogen isotope ratios were most sensitive to

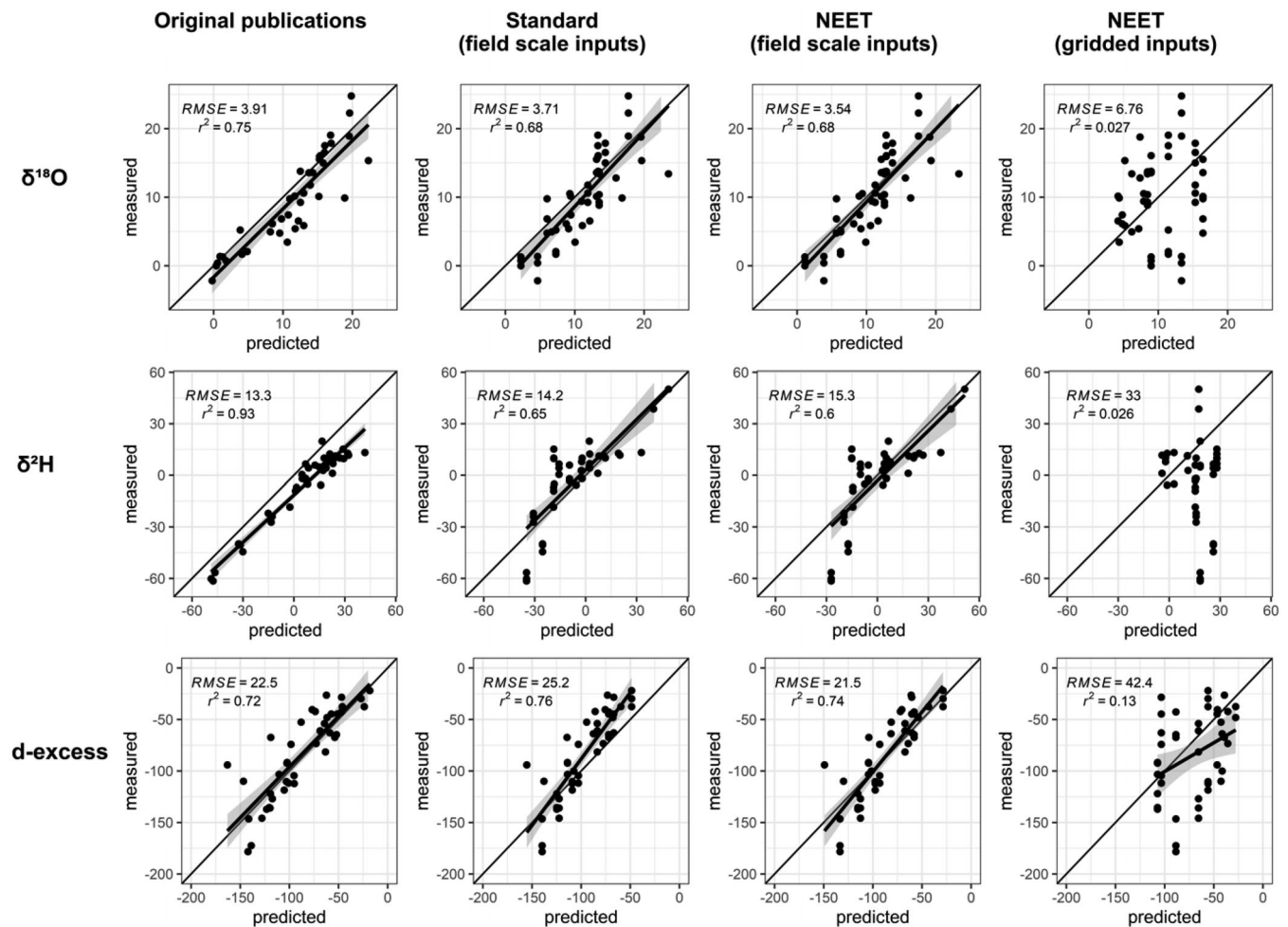


**FIGURE 6** Comparison of predicted leaf water values with observations (observations from Cernusak et al., 2016, 2022; Munksgaard et al., 2017). The first column shows the original publications' Craig-Gordon two-pool predictions using field scale inputs (short term RH, leaf temperature and xylem water isotope ratios) and individual estimations of  $\epsilon_k$  for each measurement. The second and third columns show predictions from the standard and NEET model, respectively, using field scale inputs and averaged values for  $\epsilon_k$ . The fourth column shows NEET model predictions using gridded inputs of 30 year average annual climate and annual precipitation isotope ratios (Hollins et al., 2018). All values are in ‰ VSMOW. The 1:1 relationship between predicted and measured values is shown as a black line. Linear fits to the data are shown where significant ( $p < 0.05$ ).

source water inputs and improved performance in terms of RMSE and  $r^2$  did not always lead to a smaller bias or a slope closer to one.

Measured xylem water isotope ratios (Cernusak et al., 2016, 2022) were highly variable and did not correlate with modelled annual precipitation isotope ratios from Hollins et al. (2018) (SI Figure S7). The mismatch in presumed versus measured source water values explains 16% of the variation between measured and modelled (NEET - Gridded)  $\delta^{18}\text{O}_{\text{lw}}$  and 51% of the variation between measured and modelled (NEET - Gridded)  $\delta^2\text{H}_{\text{lw}}$  models (SI Figure S8).

Cherry juice isotope ratios (SI Table S1) were compared to modelled leaf water values (Figure 8). Modelled values using long-term average inputs correlated better with cherry juice observation than they did with leaf water observations. All models with gridded input data showed higher  $r^2$  values and lower RMSEs than they did for the leaf water comparisons (Figures 6 and 7). The NEET model was the best at predicting cherry juice values with the highest  $r^2$

values and lowest RMSE of all the models for  $\delta^{18}\text{O}$ ,  $\delta^2\text{H}$ , and  $d$ -excess. Using monthly long-term average climate data for December/January or for the whole growing season instead of long-term annual climate data to make predictions resulted in somewhat better  $r^2$  values, but significantly worse RMSE values and bias (data not shown). Interannual differences in Victorian cherry juice isotope ratios for the 2018 and 2019 growing season are evident. Although the two Victorian sites were in close proximity, the 2018 values were significantly lower (average  $\pm$  standard deviation:  $\delta^{18}\text{O} = 2.3 \pm 0.4\text{‰}$ ;  $\delta^2\text{H} = 7 \pm 1\text{‰}$ ) than the 2019 values ( $\delta^{18}\text{O} = 6.9 \pm 0.4\text{‰}$ ;  $\delta^2\text{H} = 17 \pm 1\text{‰}$ ) (SI Table S1, Figure 8). These differences correspond to differences in climate between the two growing seasons, with the 2018 summer having higher than average rainfall, and the 2019 summer having lower than average rainfall for the site (Australian Bureau of Meteorology).

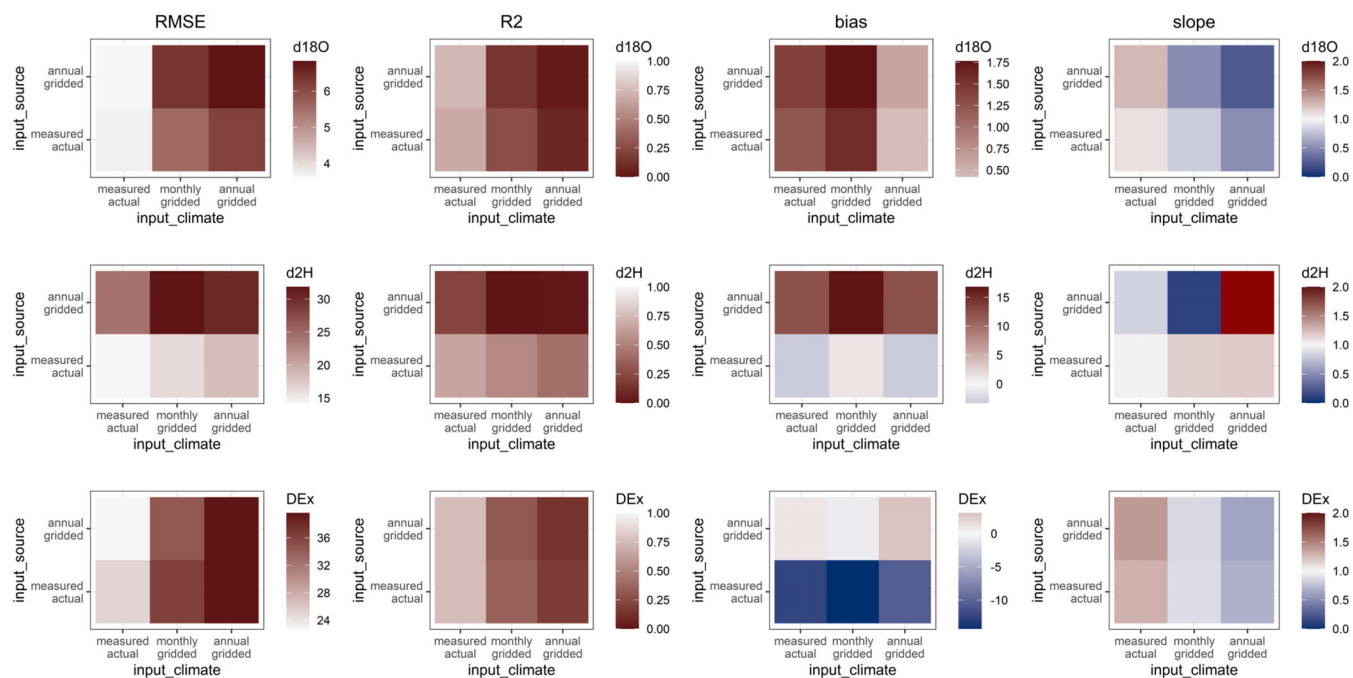


**FIGURE 7** Comparisons of model performance for predicting leaf water observations using the NEET model and combinations of actual and gridded source water isotope ratio and actual and gridded (monthly or annual) climate inputs.

Observations of oxygen isotope ratios of leaf cellulose (Cheesman & Cernusak, 2017) were compared to modelled leaf water values. Cellulose is enriched in  $^{18}\text{O}$  relative to water used in biosynthesis by up to 27‰ (Sternberg & DeNiro, 1983; Yakir & DeNiro, 1990). Thus, the predicted cellulose values in Figure 8 are adjusted from  $\delta^{18}\text{O}_{\text{lw}}$  by 27‰. We note that this enrichment is often reduced through post-photosynthetic exchange with xylem water (Cheesman & Cernusak, 2017). However, for leaves, the water used in cellulose synthesis would be from close to the sites of evaporation, rather than the bulk leaf water estimated here with two-pool mixing. Thus, the bulk leaf water values estimated here using two-pool mixing with 10% source water mimic the effect of post-photosynthetic exchange. Cellulose oxygen isotope ratios were highly correlated with modelled cellulose  $\delta^{18}\text{O}$  values, with  $r^2$  values  $>0.7$ . Both the standard and the NEET models performed similarly and better than the West et al. (2008) model, with RMSE  $<2.2\%$  (Figure 8, bottom row).

## 4 | DISCUSSION

### 4.1 | New Australian isoscapes differ from previous global isoscapes

The Australian leaf water isoscapes produced here exhibit a similar spatial pattern to the previous global leaf water isoscapes (West et al., 2008) of a general enrichment in  $\delta^{18}\text{O}$  and  $\delta^2\text{H}$  values of leaf water towards the centre of Australia (Figure 3). This pattern reflects the strong influence of relative humidity (Figure 2b) on leaf water

enrichment (Roden & Ehleringer, 1999) and the relatively small range in annual average precipitation isotope ratios (Figure 2c). While the broad patterns remain similar, there are several important differences in the new models (Table 1) that together improve the relevance and accuracy of modelled leaf water.

The new Australian isoscapes were calculated at a higher resolution ( $\sim 5$  km) than the global isoscapes ( $\sim 17$  km) and therefore better capture small-scale spatial variations like those created by topography, such as the Australian Alps in southeastern Australia (SI Figure S9). The precipitation isotope inputs used here (Hollins et al., 2018) are based on more than twice as many sampling stations (15 stations; Figure 2c,d) as the global precipitation isoscape (seven stations for Australia; Bowen & Revenaugh, 2003) and improve the coverage and calibration for inland Australia. Relative humidity inputs in the Australian isoscapes are daytime average values, which more accurately reflect the conditions when plant stomata are open and transpiration is occurring, rather than 24-h average values that were used in the global models. The estimation of kinetic fractionation during diffusion through the stomata and boundary layer ( $\epsilon_k$ ) in this study was empirically derived from hundreds of measurements from Australian plants (Cernusak et al., 2022), rather than theoretically derived (Cappa et al., 2003; Merlivat, 1978) as in West et al. (2008), making it more relevant for Australian ecosystems.

The updated input parameters contributed to varying degrees and in different ways to the overall differences between the new standard and previous global isoscapes (West et al., 2008). For leaf water  $\delta^{18}\text{O}_{\text{lw}}$  and  $d$ -excess, the updated climate and precipitation isotope inputs caused relatively small (Figure 5a,c) but spatially heterogeneous (Figure S6d,f,g,i) differences while updated  $\epsilon_k$  values produced

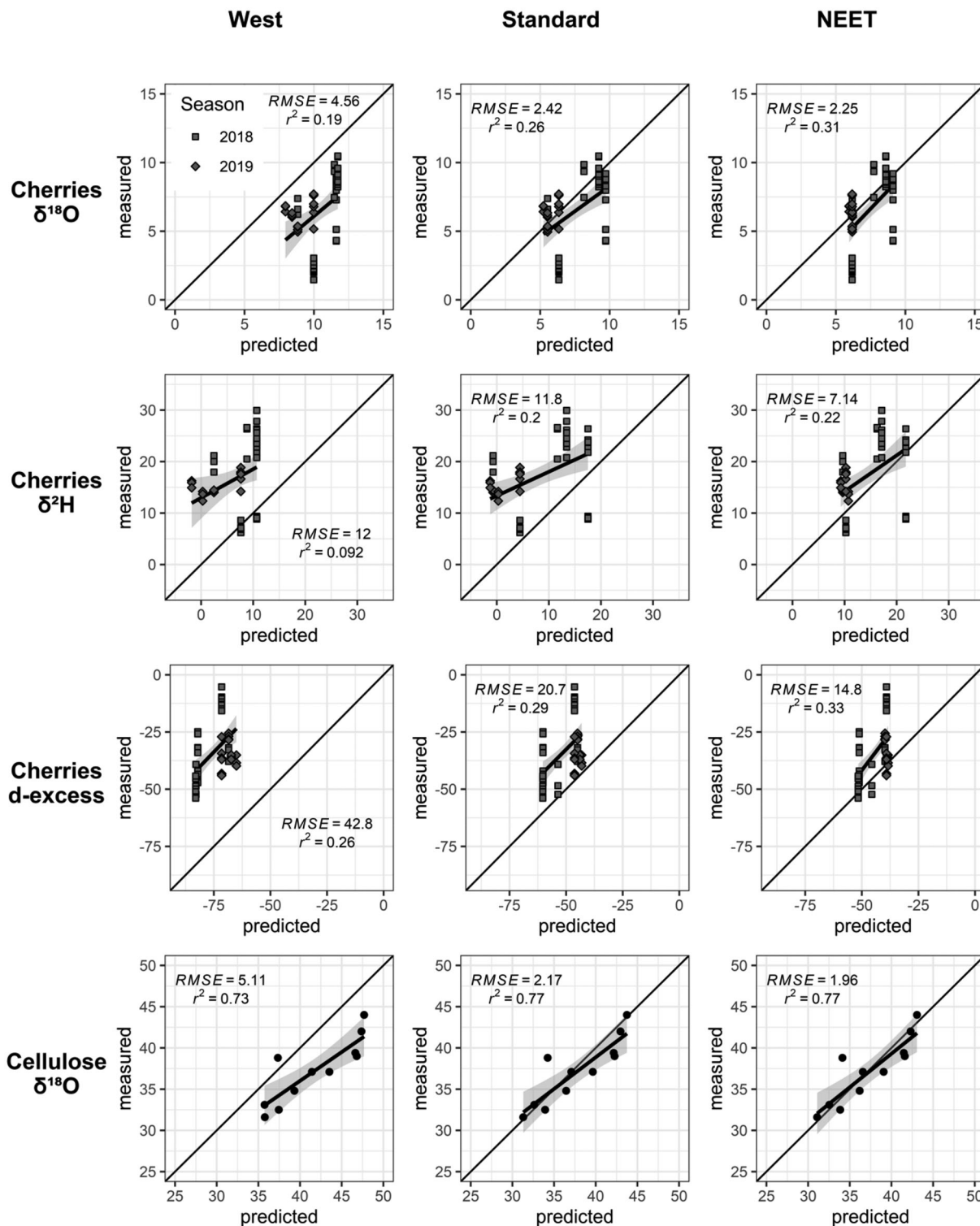


**FIGURE 8** Comparison of predicted leaf water values with observations for cherry juice (observations from Stockmann et al., 2021), and leaf cellulose (observations from Cheesman & Cernusak, 2017) for  $\delta^{18}O_{lw}$ ,  $\delta^2H_{lw}$  and  $d$ -excess. Growing season for cherries is indicated for 2018 (squares) and 2019 (diamonds). Note that for cellulose (bottom row), the predicted cellulose  $\delta^{18}O$  value is estimated as  $\delta^{18}O_{lw} + 27\%$ . All values are in ‰ VSMOW. The 1:1 relationship between predicted and measured values is shown as a black line. Linear fits to the data are shown where significant ( $p < 0.05$ ).

large (Figure 5a,c) but spatially homogenous differences (Figure S6j,l). For  $\delta^2H_{lw}$ , climate, precipitation isotope inputs and  $\epsilon_k$  all contributed substantially to the net difference (Figure 5b). The greater effect of

precipitation isotope inputs on  $\delta^2H_{lw}$  than  $\delta^{18}O_{lw}$  reflects the greater influence of atmospheric water vapour on  $\delta^2H_{lw}$  than  $\delta^{18}O_{lw}$  values (Cernusak et al., 2022).

In addition to improving the parameterisation for relative humidity and  $\epsilon_k$ , the NEET model included a correction for water vapour non-equilibrium (Fiorella et al., 2019) and an empirical leaf–air temperature relationship. These changes led to both positive and negative differences from the standard model spanning an absolute range of 2.6‰, 14.6‰ and 17.8‰ for  $\delta^{18}\text{O}_{\text{lw}}$ ,  $\delta^2\text{H}_{\text{lw}}$  and  $d$ -excess, respectively (Figure 4). For hydrogen, large positive differences between NEET and the standard model were seen in tropical northern Australia and Tasmania where the largest non-equilibrium vapour corrections were applied (SI Figure S1). For oxygen, large positive differences occurred in Tasmania, but only small negative differences were found in tropical northern Australia, in spite of similar spatial distributions of non-equilibrium vapour corrections for oxygen and hydrogen (Figure 2e; SI Figure S1). The smaller  $\delta^{18}\text{O}_{\text{lw}}$  differences in northern Australia reflect the counter-balancing effect of differences in leaf temperature estimation in the two models. Differences in leaf temperature in the NEET and standard model are the greatest at high temperatures (SI Figure S2), leading to the largest temperature-induced differences expected in the tropical north. In addition, temperature has a larger influence on  $\delta^{18}\text{O}_{\text{lw}}$  than  $\delta^2\text{H}_{\text{lw}}$  (Cernusak et al., 2022) which would explain why the counterbalancing effect is larger for oxygen than hydrogen.

## 4.2 | Evaluation of accuracy of New Australian isoscapes

The standard and NEET models successfully predicted leaf water observations when short-term climate and xylem water isotope values were used as inputs (Figure 6), reaffirming that Craig-Gordon two-pool models and the specific formulations used here broadly capture the key processes influencing leaf water isotope ratios (Cernusak et al., 2016). As expected, instantaneous isotope observations did not agree with model predictions using long-term average gridded climate and source water inputs due to differences in short- and long-term conditions. Climate varies diurnally, seasonally, and interannually and ground water, storms and evaporated surface waters are all factors that cause variation in the isotopic composition of the plant's source water (Oerter & Bowen, 2019). As a result, the measured source (xylem) water (Cernusak et al., 2016, 2022; Munksgaard et al., 2017) bears no relationship to the long-term amount-weighted average precipitation isotope ratios (SI Figure S7). This mismatch in source water isotope ratios explained only 16% of the mismatch between measured and modelled leaf water values for oxygen while explaining 51% for hydrogen (SI Figure S8). The larger impact of source water values on hydrogen isotope ratios is seen in the sensitivity of model performance to source water input data quality (Figure 7) and is consistent with the larger influence of atmospheric vapour on hydrogen isotope ratios of leaf water (Cernusak et al., 2022). Oxygen isotope ratios and  $d$ -excess of leaf water, on the other hand, are more sensitive to the climate input data quality used (Figure 7), reflecting the greater influence of relative humidity (Cernusak et al., 2022).

The high variability in short-term observations of leaf water isotope ratios makes them ill-suited for generating long-term average leaf water isoscapes using geostatistical approaches. For organisms incorporating leaf water during growth, it is the time-integrated average that is most relevant. To examine the accuracy of the process-based models used here for predicting the average isotopic composition of leaf water, all three models were compared to observed isotope ratios of leaf cellulose and cherry juice. Both cellulose and cherry juice had much stronger correlations with modelled leaf water values than the observations of leaf water did, with higher  $r^2$  and lower RMSE values (Figures 6 and 8). Regressions between measured and predicted values for leaf cellulose and cherries also had slopes much closer to one (0.7–1.1 for  $\delta^{18}\text{O}_{\text{lw}}$ ; 0.5–0.7 for  $\delta^2\text{H}_{\text{lw}}$  and 1–1.3 for  $d$ -excess) than for leaf water. Thus, modelled leaf water values provide a more accurate representation of isotope ratios of biological materials that integrate over longer periods of time than they do for instantaneous leaf water samples. Materials that would be best represented by the isoscapes developed here would include plant tissues as well as herbivore tissues of organisms that use plant water as a substantive source of body water, such as kangaroos, koalas and emus (Ayliffe & Chivas, 1990; DeSantis & Hedberg, 2016; Miller & Fogel, 2016; Murphy et al., 2007).

The data-model comparisons enable evaluation of the relative accuracy of the different models. Both of the new Australian isoscapes (standard and NEET) predicted the cherry juice and cellulose observations more accurately than the previous global model (Figure 8). Moreover, the NEET model provides a better fit to the cherry and leaf cellulose data than the standard model, indicating that adjustments made to leaf temperature and water vapour have improved the accuracy of predictions.

In addition to spatial variability, there is also significant temporal variability in leaf water isotope ratios at any one location on multiple scales: (a) seasonal changes (e.g., between winter and summer averages); (b) daily changes (e.g., between 9 am and 3 pm averages); and (c) deviations of actual conditions from long-term means. The variability observed in the cherry juice isotope ratios between the wetter than average 2018 growing season and the dryer than average 2019 growing seasons demonstrate the impact of such deviations from average climate. Although the magnitude of the effects of (c) cannot be assessed with the climate dataset used here, our results do allow for a rough estimation of long-term average seasonal and daily variation, and comparison of the magnitude of temporal and spatial variations. Generally, spatial variability is approximately twice as large as temporal variability on both seasonal and daily time scales (Table 3). This provides some constraints on the applicability of the long-term average isoscape presented here. Biological tissues that integrate the leaf water signature over a year or longer (e.g., kangaroo bones) would not be affected by the seasonal and daily variations (a and b) and therefore, the long-term annual average isoscapes are appropriate for interpretation of measurements from such tissue, although (c) would still be relevant. If a biological tissue integrates over months (e.g., cherries), monthly resolved long-term average isoscapes might improve predictions. If biological tissue only integrates the leaf water

signature over a sub-daily timescale (e.g., leaf water itself), the daily temperature and relative humidity cycles would need to be included in the isoscape modelling to yield an accurate prediction.

### 4.3 | Implications, applications and future work

This paper is the first to develop continental-scale leaf water oxygen, hydrogen and *d*-excess isoscapes that incorporate empirical and region-specific vegetation parameters and correct for non-equilibrium water vapour isotopic composition. The resulting isoscapes represent a significant improvement over previous global isoscapes in terms of better predicting spatial variations in the composition of plant tissues. The largest improvements were seen in hydrogen isotope ratios and *d*-excess, which are most sensitive to water vapour composition (Cernusak et al., 2022). The methodology that is applied here to Australia is relevant to developing regionally grounded models that account for vapour-disequilibrium around the world. These more accurate predictions of leaf water composition are needed to trace the movement of water along the soil–plant–atmosphere continuum.

The isoscapes produced here use process-based models to predict long-term average leaf water values that are reflected in organic tissues of plants and animals. These predictions enable analysis of spatial variations relevant for tracking and tracing biological materials in ecological, agricultural and forensic studies. For example, leaf water isotopes support research into the autecology of vertebrates such as kangaroos, koalas and emus (Ayliffe & Chivas, 1990; DeSantis & Hedberg, 2016; Miller & Fogel, 2016; Murphy et al., 2007), the interconnections in food webs (Vander Zanden et al., 2016) and the ecology of invasive species (McCue et al., 2020). In addition, these predictions are directly relevant for geographic provenancing for forensics and food authentication (Camin et al., 2017; Gentile et al., 2015). Finally, advances in our appreciation for the role of leaf water in influencing the isotopic composition of atmospheric moisture (Li et al., 2016; Simonin et al., 2014; Zhao et al., 2014) suggest that accurate leaf water isoscapes are also relevant to atmospheric modelling.

Recent research used leaf water isoscapes and plant physiological models to predict oxygen isotope ratios of strawberries from across Europe (Cueni et al., 2021). Their leaf water model assumed that atmospheric vapour was in equilibrium with precipitation, as occurs immediately after a rainfall (Welp et al., 2008), because strawberries are well-watered crops. Their study found that model predictions for oxygen isotope ratios were greatly improved by using climate data for the year and season of growth because of the strong impact of climate on leaf water isotope ratios, and the inter- and intra-annual variability in climate (Cueni et al., 2021). Similarly, we find that for the location in Victoria, a wetter than average growing season caused cherry juice isotope ratios to be low while a dryer than average growing season caused them to be high. The next step in improving the NEET model will be to use time-resolved climate data, with the ability to predict monthly, seasonal, and annual leaf water isoscapes through time. These time-resolved isoscapes will improve predictions by

capturing shorter term variations in climate that are especially critical for biological materials that form sub annually. More accurate climate inputs will most significantly improve oxygen isotope and *d*-excess predictions that are most sensitive to climate inputs (Figure 7). Hydrogen isotope predictions, on the other hand, are most sensitive to source water isotopic inputs (Figure 7) and better estimations of source water isotopic composition would benefit future hydrogen isoscapes for leaf water. An additional improvement for annual isoscapes of leaf water will be to weight them by net primary productivity (NPP) to capture the seasonal variations in photosynthesis and transpiration, and to better characterize the leaf water available for ingestion by herbivores.

To make the standard and NEET isoscapes produced here available for use by the research community, leaf water enrichments ( $\Delta_e$ ) and isotope ratios ( $\delta^{18}\text{O}_{\text{lw}}$ ,  $\delta^2\text{H}_{\text{lw}}$  and *d*-excess) for any location in Australia can be queried, and gridded data downloaded through the Australian Leaf Water Isoscape Portal (ALWI) available at <https://doi.org/10.48610/f15ea0a> or <https://shiny.rcc.uq.edu.au/ALWI/>.

## 5 | CONCLUSIONS

The leaf water  $\delta^{18}\text{O}$ ,  $\delta^2\text{H}$  and *d*-excess isoscapes developed here incorporate recent advances in knowledge and regionally specific parameters to improve the accuracy and resolution of predictions relative to the previously available global isoscapes (West et al., 2008). Regionally specific parameters included Australian-specific precipitation isoscapes (Hollins et al., 2018), empirically estimated kinetic fractionation ( $\epsilon_k$ ) values and an empirical leaf-to-air temperature relationship (Cernusak et al., 2016; Cernusak et al., 2022; Munksgaard et al., 2017). The use of the new  $\epsilon_k$  values led to large differences from the previous global isoscapes, especially for  $\delta^{18}\text{O}_{\text{lw}}$  and *d*-excess. In addition, non-equilibrium water vapour isotope ratios were estimated using offsets from Fiorella et al. (2019). The correction for non-equilibrium water vapour had a larger effect on  $\delta^2\text{H}_{\text{lw}}$  than  $\delta^{18}\text{O}_{\text{lw}}$ , which is consistent with the greater influence of water vapour isotopic composition on  $\delta^2\text{H}_{\text{lw}}$  than on  $\delta^{18}\text{O}_{\text{lw}}$  (Cernusak et al., 2022).

The aim of this research was to develop region-specific mechanistic models that would enable accurate prediction of long-term average leaf water composition for comparison with plant and animal tissues. The two models developed here more accurately predicted the isotope ratios of leaf cellulose and cherry juice than the previous global model, with the NEET model performing better than the standard model.

The NEET isoscapes provide the most accurate representation available of long-term average leaf water isotope ratios for Australia. These isoscapes enable isotopic tracing of leaf water into plants and animals to support research in ecohydrology, atmospheric science, isotope ecology, agriculture and forensics.

## ACKNOWLEDGEMENTS

The authors would like to acknowledge Uta Stockmann and Mark Farrell for their design and development of the work supporting the

cherry data referred to in this manuscript. The cherry analysis was supported by the Science and Industry Endowment Fund. We would like to thank J. West for providing gridded data for the published global leaf water isoscapes, R. Fiorella for providing gridded data for water vapour bias correction, D. Ray for useful discussions regarding climate datasets, A. Hellicar for useful discussions regarding modelling and G. Bowen for assistance during early explorations of leaf water isoscapes using ISO-MAP. Open access publishing facilitated by The University of Queensland, as part of the Wiley - The University of Queensland agreement via the Council of Australian University Librarians.

## DATA AVAILABILITY STATEMENT

R code for leaf water modelling has been made available in Supporting Information. Gridded isoscapes and data for individual locations available at Australian Leaf Water Isoscape Portal (ALWI) at <https://doi.org/10.48610/f15ea0a> or <https://shiny.rcc.uq.edu.au/ALWI/>.

## ORCID

Francesca A. McInerney  <https://orcid.org/0000-0002-2020-6650>

Christoph Gerber  <https://orcid.org/0000-0003-4339-5746>

Lucas A. Cernusak  <https://orcid.org/0000-0002-7575-5526>

Athina Puccini  <https://orcid.org/0000-0002-1023-9088>

Steve Szarvas  <https://orcid.org/0000-0002-2432-3029>

Tanoj Singh  <https://orcid.org/0000-0002-0413-1935>

Nina Welti  <https://orcid.org/0000-0001-9966-5915>

## REFERENCES

- Ayliffe, L. K., & Chivas, A. R. (1990). Oxygen isotope composition of the bone phosphate of Australian kangaroos: Potential as a palaeoenvironmental recorder. *Geochimica et Cosmochimica Acta*, 54(9), 2603–2609. [https://doi.org/10.1016/0016-7037\(90\)90246-H](https://doi.org/10.1016/0016-7037(90)90246-H)
- Barbour, M. M., Loucos, K. E., Lockhart, E. L., Shrestha, A., McCallum, D., Simonin, K. A., Song, X., Griffani, D. S., & Farquhar, G. D. (2021). Can hydraulic design explain patterns of leaf water isotopic enrichment in C3 plants? *Plant, Cell & Environment*, 44(2), 432–444. <https://doi.org/10.1111/pce.13943>
- BoM. (2005). Temperature: Mean, maximum and minimum monthly, seasonal, and annual temperature gridded data (base climatological data sets, 1961 to 1990). *Australian Bureau of Meteorology* <http://www.bom.gov.au/metadata/19115/ANZCW0503900354>
- BoM. (2009). Relative humidity: Mean monthly and mean annual relative humidity data (base climatological dataset, 1976–2005). *Australian Bureau of Meteorology* <http://www.bom.gov.au/metadata/19115/ANZCW0503900359>
- Bowen, G. J. (2010a). Isoscapes: Spatial pattern in isotopic biogeochemistry. *Annual Review of Earth and Planetary Sciences*, 38, 161–187.
- Bowen, G. J. (2010b). Statistical and geostatistical mapping of precipitation water isotope ratios. In J. B. West, G. J. Bowen, T. E. Dawson, & K. P. Tu (Eds.), *Isoscapes: Understanding movement, pattern and process on earth through isotope mapping* (pp. 139–160). Springer.
- Bowen, G. J., & Revenaugh, J. (2003). Interpolating the isotopic composition of modern meteoric precipitation. *Water Resources Research*, 39(10), 1299. <https://doi.org/10.1129/2003WR002086>
- Camin, F., Boner, M., Bontempo, L., Fahl-Hassek, C., Kelly, S. D., Riedl, J., & Rossmann, A. (2017). Stable isotope techniques for verifying the declared geographical origin of food in legal cases. *Trends in Food Science & Technology*, 61, 176–187. <https://doi.org/10.1016/j.tifs.2016.12.007>
- Cappa, C. D., Hendricks, M. B., DePaulo, D. J., & Cohen, R. C. (2003). Isotopic fractionation of water during evaporation. *Journal of Geophysical Research*, 108, 4525. <https://doi.org/10.1029/2003JD003597>
- Cernusak, L. A., Barbeta, A., Bush, R. T., Eichstaedt, R., Ferrio, J. P., Flanagan, L. B., Gessler, A., Martín-Gómez, P., Hirl, R. T., Kahmen, A., Keitel, C., Lai, C.-T., Munksgaard, N. C., Nelson, D. B., Ogee, J., Roden, J. S., Schnyder, H., Voelker, S.L., Wang, L., ... Cuntz, M. (2022). Do 2H and 18O in leaf water reflect environmental drivers differently? *New Phytologist*, 235, 41–51. <https://doi.org/10.1111/nph.18113>
- Cernusak, L. A., Barbour, M. M., Arndt, S. K., Cheesman, A. W., English, N. B., Feild, T. S., Helliker, B. R., Holloway-Phillips, M. M., Holtum, J. A. M., Kahmen, A., McInerney, F. A., Munksgaard, N. C., Simonin, K. A., Song, X., Stuart-Williams, H., West, J. B., & Farquhar, G. D. (2016). Stable isotopes in leaf water of terrestrial plants. *Plant, Cell & Environment*, 39(5), 1087–1102. <https://doi.org/10.1111/pce.12703>
- Cheesman, A. W., & Cernusak, L. A. (2017). Infidelity in the outback: Climate signal recorded in  $\Delta 18\text{O}$  of leaf but not branch cellulose of eucalypts across an Australian aridity gradient. *Tree Physiology*, 37(5), 554–564. <https://doi.org/10.1093/treephys/tpw121>
- Craig, H., & Gordon, L. I. (1965). Deuterium and oxygen-18 variations in the ocean and the marine atmosphere. In E. Tongiorgi (Ed.), *Proceedings of the third Spoleto conference on stable isotopes in oceanographic studies and paleotemperatures* (pp. 9–130), CNR-Laboratorio di Geologia Nucleare.
- Crisp, M. D., Laffan, S., Linder, H. P., & Monro, A. N. N. A. (2001). Endemism in the Australian flora. *Journal of Biogeography*, 28, 183–198.
- Cueni, F., Nelson, D. B., Boner, M., & Kahmen, A. (2021). Using plant physiological stable oxygen isotope models to counter food fraud. *Scientific Reports*, 11(1), 17314. <https://doi.org/10.1038/s41598-021-96722-9>
- Daniel Bryant, J., & Froelich, P. N. (1995). A model of oxygen isotope fractionation in body water of large mammals. *Geochimica et Cosmochimica Acta*, 59(21), 4523–4537. [https://doi.org/10.1016/0016-7037\(95\)00250-4](https://doi.org/10.1016/0016-7037(95)00250-4)
- Dansgaard, W. (1964). Stable isotopes in precipitation. *Tellus*, 16, 436–438.
- Davies, J., Poulsen, L., Schulte-Herbrüggen, B., Mackinnon, K., Crawhall, N., Henwood, W. D., Dudley, N., Smith, J., & Gudka, M. (2012). *Conserving dryland biodiversity*. International Union for the conservation of nature. 84p.
- DeSantis, L. R. G., & Hedberg, C. (2016). Stable isotope ecology of the koala (*Phascolarctos cinereus*). *Australian Journal of Zoology*, 64(5), 353–359. <https://doi.org/10.1071/ZO16057>
- Dong, N., Prentice, I. C., Harrison, S. P., Song, Q. H., & Zhang, Y. P. (2017). Biophysical homeostasis of leaf temperature: A neglected process for vegetation and land-surface modelling. *Global Ecology and Biogeography*, 26, 998–1007. <https://doi.org/10.1111/geb.12614>
- Ehleringer, J. R., Schwinning, S., & Gebauer, R. (1999). Water use in arid land ecosystems. In M. C. Press (Ed.), *Advances in physiological plant ecology* (pp. 347–365). Blackwell Science.
- Farquhar, G. D., Hubick, K. T., Condon, A. G., & Richards, R. A. (1989). Carbon isotope fractionation and plant water-use efficiency. In P. W. Rundel, J. R. Ehleringer, & K. A. Nagy (Eds.), *Stable isotopes in ecological research* (pp. 21–46). Springer-Verlag.
- Feldman, A. F., Chulakadabba, A., Gianotti, D. J. S., & Entekhabi, D. (2021). Landscape-scale plant water content and carbon flux behavior following moisture pulses: From dryland to Mesic environments. *Water Resources Research*, 57(1), e2020WR027592. <https://doi.org/10.1029/2020wr027592>
- Fiorella, R. P., West, J. B., & Bowen, G. J. (2019). Biased estimates of the isotope ratios of steady-state evaporation from the assumption of equilibrium between vapour and precipitation. *Hydrological Processes*, 33(19), 2576–2590. <https://doi.org/10.1002/hyp.13531>
- Gat, J. R. (2000). Atmospheric water balance—The isotopic perspective. *Hydrological Processes*, 14(8), 1357–1369. [https://doi.org/10.1002/1099-1085\(20000615\)14:8<1357::AID-HYP986>3.0.CO;2-7](https://doi.org/10.1002/1099-1085(20000615)14:8<1357::AID-HYP986>3.0.CO;2-7)



- Gentile, N., Siegwolf, R. T. W., Esseiva, P., Doyle, S., Zollinger, K., & Delémont, O. (2015). Isotope ratio mass spectrometry as a tool for source inference in forensic science: A critical review. *Forensic Science International*, 251, 139–158. <https://doi.org/10.1016/j.forsciint.2015.03.031>
- Hoffmann, G., Cuntz, M., Weber, C., Ciais, P., Friedlingstein, P., Heimann, M., Jouzel, J., Kaduk, J., Maier-Reimer, E., Seibt, U., & Six, K. (2004). A model of the Earth's dole effect. *Global Biogeochemical Cycles*, 18(1). <https://doi.org/10.1029/2003GB002059>
- Hollins, S. E., Hughes, C. E., Crawford, J., Cendón, D. I., & Meredith, K. T. (2018). Rainfall isotope variations over the Australian continent—Implications for hydrology and isoscape applications. *Science of the Total Environment*, 645, 630–645. <https://doi.org/10.1016/j.scitotenv.2018.07.082>
- Horita, J., & Wesolowski, D. J. (1994). Liquid-vapor fractionation of oxygen and hydrogen isotopes of water from the freezing to the critical temperature. *Geochimica et Cosmochimica Acta*, 58(16), 3425–3437.
- Houerou, G., Kelly, S. D., & Dennis, M. J. (1999). Determination of the oxygen-18/oxygen-16 isotope ratios of sugar, citric acid and water from single strength orange juice. *Rapid Communications in Mass Spectrometry*, 13, 1257–1262.
- Jones, D., Wang, Q. W., & Fawcett, R. (2009). High-quality spatial climate data-sets for Australia. *Australian Meteorological Magazine*, 58, 233–248. <https://doi.org/10.22499/2.5804.003>
- Kohn, M. J., Schoeninger, M. J., & Valley, J. W. (1996). Herbivore tooth oxygen isotope compositions: Effects of diet and physiology. *Geochimica et Cosmochimica Acta*, 60, 3889–3896.
- Koziet, J., Rossmann, A., Martin, G. J., & Johnson, P. (1995). Determination of the O-18 and deuterium content of fruit and vegetable juice water—An European inter-laboratory comparison study. *Analytica Chimica Acta*, 302, 29–37.
- Leaney, F., Osmond, C., Allison, G., & Ziegler, H. (1985). Hydrogen-isotope composition of leaf water in C3 and C4 plants: Its relationship to the hydrogen-isotope composition of dry matter. *Planta*, 164, 215–220.
- Lloyd, J., & Farquhar, G. D. (1994). <sup>13</sup>C discrimination during CO<sub>2</sub> assimilation by the terrestrial biosphere. *Oecologia*, 99, 201–215.
- Luz, B., Barkan, E., Yam, R., & Shemesh, A. (2009). Fractionation of oxygen and hydrogen isotopes in evaporating water. *Geochimica et Cosmochimica Acta*, 73(22), 6697–6703. <https://doi.org/10.1016/j.gca.2009.08.008>
- McCue, M. D., Javal, M., Clusella-Trullas, S., Le Roux, J. J., Jackson, M. C., Ellis, A. G., Richardson, D. M., Valentine, A. J., & Terblanche, J. S. (2020). Using stable isotope analysis to answer fundamental questions in invasion ecology: Progress and prospects. *Methods in Ecology and Evolution*, 11(2), 196–214. <https://doi.org/10.1111/2041-210X.13327>
- Merlivat, L. (1978). Molecular diffusivities of H<sub>2</sub><sup>18</sup>O in gases. *Journal of Chemical Physics*, 69, 2864–2871.
- Miller, G. H., & Fogel, M. L. (2016). Calibrating δ18O in *Dromaius novaehollandiae* (emu) eggshell calcite as a paleo-aridity proxy for the quaternary of Australia. *Geochimica et Cosmochimica Acta*, 193, 1–13. <https://doi.org/10.1016/j.gca.2016.08.004>
- Munksgaard, N. C., Cheesman, A. W., English, N. B., Zwart, C., Kahmen, A., & Cernusak, L. A. (2017). Identifying drivers of leaf water and cellulose stable isotope enrichment in eucalyptus in northern Australia. *Oecologia*, 183(1), 31–43. <https://doi.org/10.1007/s00442-016-3761-8>
- Murphy, B. P., & Bowman, D. M. J. S. (2007). Seasonal water availability predicts the relative abundance of C3 and C4 grasses in Australia. *Global Ecology and Biogeography*, 16(2), 160–169. <https://doi.org/10.1111/j.1466-8238.2006.00285.x>
- Murphy, B. P., Bowman, D. M. J. S., & Gagan, M. K. (2007). The interactive effect of temperature and humidity on the oxygen isotope composition of kangaroos. *Functional Ecology*, 21(4), 757–766. <https://doi.org/10.1111/j.1365-2435.2007.01284.x>
- New, M., Lister, D., Hulme, M., & Makin, I. (2002). A high-resolution data set of surface climate over global land areas. *Climate Research*, 21, 1. <https://doi.org/10.3354/cr021001>
- Oerter, E. J., & Bowen, G. J. (2019). Spatio-temporal heterogeneity in soil water stable isotopic composition and its ecohydrologic implications in semiarid ecosystems. *Hydrological Processes*, 33(12), 1724–1738. <https://doi.org/10.1002/hyp.13434>
- Oki, T., & Kanae, S. (2006). Global hydrological cycles and world water resources. *Science*, 313(5790), 1068–1072. <https://doi.org/10.1126/science.1128845>
- Právělie, R. (2016). Drylands extent and environmental issues. A global approach. *Earth-Science Reviews*, 161, 259–278. <https://doi.org/10.1016/j.earscirev.2016.08.003>
- Rockström, J., & Falkenmark, M. (2000). Semiarid crop production from a hydrological perspective: Gap between potential and actual yields. *Critical Reviews in Plant Sciences*, 19(4), 319–346. <https://doi.org/10.1080/07352680091139259>
- Roden, J. S., & Ehleringer, J. R. (1999). Observations of hydrogen and oxygen isotopes in leaf water confirm the Craig-Gordon model under wide-ranging environmental conditions. *Plant Physiology*, 120, 1165–1173.
- Simonin, K. A., Link, P., Rempe, D., Miller, S., Oshun, J., Bode, C., Dietrich, W. E., Fung, I., & Dawson, T. E. (2014). Vegetation induced changes in the stable isotope composition of near surface humidity. *Ecohydrology*, 7(3), 936–949. <https://doi.org/10.1002/eco.1420>
- Song, X., Loucos, K. E., Simonin, K. A., Farquhar, G. D., & Barbour, M. M. (2015). Measurements of transpiration isotopologues and leaf water to assess enrichment models in cotton. *New Phytologist*, 206, 637–646.
- Sternberg, L., & DeNiro, M. (1983). Biogeochemical implications of the isotopic equilibrium fractionation factor between the oxygen atoms of acetone and water. *Geochimica et Cosmochimica Acta*, 47(12), 2271–2274. [https://doi.org/10.1016/0016-7037\(83\)90049-2](https://doi.org/10.1016/0016-7037(83)90049-2)
- Stockman, U., Smith, D., Dominik, S., Barlow, R., Camtepe, S., Chan, J., Crawford, J., Ding, M., Farrell, M., Guan, X., Hellicar, A., Hughes, C., Kaafar, D., Lu, Q., Marvanek, S., Puccini, A., Rakotoarivelo, T., Reverter, A., Singh, T., ... Zhu, L. (2021). Work package 3: Biological origin in the supply chain integrity phase 2 initiative. Technical Report, CSIRO, Australia.
- UN. (2011). *Global drylands: A UN system-wide response*. United Nations Environmental Management Group Report.
- Vander Zanden, H. B., Soto, D. X., Bowen, G. J., & Hobson, K. A. (2016). Expanding the isotopic toolbox: Applications of hydrogen and oxygen stable isotope ratios to food web studies. *Frontiers in Ecology and Evolution*, 4. <https://doi.org/10.3389/fevo.2016.00020>
- Welp, L. R., Lee, X., Kim, K., Griffis, T. J., Billmark, K. A., & Baker, J. M. (2008). deltaO of water vapour, evapotranspiration and the sites of leaf water evaporation in a soybean canopy. *Plant, Cell & Environment*, 31(9), 1214–1228. <https://doi.org/10.1111/j.1365-3040.2008.01826.x>
- West, J. B., Sobek, A., & Ehleringer, J. (2008). A simplified GIS approach to modeling global leaf water isoscapes. *PLoS One*, 3(6), e2447. <https://doi.org/10.1371/journal.pone.0002447>
- Woo, J., Zhao, L., & Bowen, G. J. (2021). Streamlining geospatial data processing for isotopic landscape modeling. *Concurrency and Computation: Practice and Experience*, 33(19), e6324. <https://doi.org/10.1002/cpe.6324>
- Yakir, D., & DeNiro, M. J. (1990). Oxygen and hydrogen isotope fractionation during cellulose metabolism in *Lemna gibba* L. 1. *Plant Physiology*, 93(1), 325–332. <https://doi.org/10.1104/pp.93.1.325>
- Zhao, L., Wang, L., Liu, X., Xiao, H., Ruan, Y., & Zhou, M. (2014). The patterns and implications of diurnal variations in the d-excess of plant water, shallow soil water and air moisture. *Hydrology and Earth System Sciences*, 18(10), 4129–4151. <https://doi.org/10.5194/hess-18-4129-2014>

Zongxing, L., Qi, F., Wang, Q. J., Yanlong, K., Aifang, C., Song, Y., Yongge, L., Jianguo, L., & Xiaoyan, G. (2016). Contributions of local terrestrial evaporation and transpiration to precipitation using delta  $\delta^{18}\text{O}$  and D-excess as a proxy in Shiyang inland river basin in China. *Global and Planetary Change*, 146, 140–151. <https://doi.org/10.1016/j.gloplacha.2016.10.003>

#### SUPPORTING INFORMATION

Additional supporting information can be found online in the Supporting Information section at the end of this article.

**How to cite this article:** McInerney, F. A., Gerber, C., Dangerfield, E., Cernusak, L. A., Puccini, A., Szarvas, S., Singh, T., & Welti, N. (2023). Leaf water  $\delta^{18}\text{O}$ ,  $\delta^2\text{H}$  and *d*-excess isoscapes for Australia using region-specific plant parameters and non-equilibrium vapour. *Hydrological Processes*, 37(5), e14878. <https://doi.org/10.1002/hyp.14878>